First publ. in: Langmuir 24 (2008), 2341-2347

Crystallization as a Means for the Switching of Nanoscale Containers

Qiong Tong, Marina Krumova, Inigo Göttker-Schnetmann, and Stefan Mecking*

Chair of Chemical Materials Science, Department of Chemistry, University of Konstanz, Universitätsstr. 10, D-78457 Konstanz, Germany

Melting and crystallization are reported as a means for reversible switching of nanoscale containers. Aqueous dispersions of 10 nm particles of polyethylene with variable branching and crystallinity were prepared by catalytic polymerization with water-soluble Ni(II) complexes. Fluorescence studies of lipophilic probe molecules show that in the low-crystallinity particles they experience a more apolar environment. In crystalline particles, the amorphous portions which can accommodate guest molecules are at the periphery of the particle, such that the probe experiences the water−particle interface to some extent. The polarity experienced by the probe molecules can be switched reversibly by melting and crystallization of the individual dispersed particles. The temperature at which this occurs can be adjusted via the microstructure, that is, degree of branching, of the polymer.

Introduction

The behavior of nanoscale entities toward molecular guests has been studied intensely over the past 5−10 years. Beyond fundamental interest in the properties of very small compartments, this issue is also relevant for applications such as, for example, delivery of poorly soluble drugs, controlled release of active molecules, and homogeneous incorporation of functional molecules such as dyes into solid materials or as carriers in aqueous multiphase catalysis.[1−8] Nanoscale entities with very small sizes, that is, approximately 5−20 nm, dispersed in water are of particular interest. They possess a high permeability through, for example, biological membranes, and the high ratio of the interface to the continuous surrounding medium versus the volume results in high accessibility and also colloidal stability. Water is obviously attractive as a continuous phase in view of its ubiquitous presence in nature and also in many technical applications. Various dendritic molecules have been studied as hosts for small molecules.[3,4] An amphiphilic structure with a hydrophilic periphery and a rather apolar interior can result in nonaggregated unimolecular micelle structures.[9,10] While the single-step synthesis of a hyperbranched lipophilic core has been demonstrated,[10] the dendrimer cores usually employed require multistep syntheses for their preparation. Alternatively, very small structures can be formed by aggregation of amphiphilic molecules or polymers, with linear or also branched microstructures.[11,12] Note that generally the size and structure of such aggregates will be more sensitive to external conditions such as concentration, temperature, and small changes in the composition of the solvent.

Controlled switching of the properties of the aforementioned nanoscale entities by external stimuli is desirable. To this end, pH sensitive systems have been studied. Most often, fluorescent probe molecules were employed to monitor these changes and their effects on the environment experienced by a guest molecule. Chemical hydrolysis of bonds in the carrier entities has been employed, which is irreversible.[13] By comparison, changes in polarity or aggregation number resulting from protonation can be reversible in principle (though in most cases reversibility was not demonstrated).[14] As another concept, temperature-dependent changes of the miscibility of chain segments with the liquid dispersing medium which result in a lower critical solution temperature (LCST) have been investigated.[15−19] It can be noted that in the aforementioned approaches in most cases "switching" is accompanied by aggregation and strong changes in size.

Crystallization of polymers is a ubiquitous and general phenomenon.[20−26] Surprisingly, however, crystallization and melting have not been studied in dispersed small structures suited as nanocontainers and as a means of switching the latter with respect to the properties experienced by guest molecules. This may be due in part to a lack of convenient accessibility of suitable nanoparticles to date. We report on the effect of reversible

* To whom correspondence should be addressed. E-mail: stefan.mecking@uni-konstanz.de.

(1) Caruso, F *Colloids and Colloid Assemblies*; Wiley-VCH: Weinheim, 2004
(2) Haag, R *Angew. Chem.* **2004**, *116*, 280−284 Haag, R *Angew. Chem., Int. Ed* **2004**, *43*, 278−282
(3) Bosman, A W ; Janssen, H M ; Meijer, E W *Chem. Rev.* **1999**, *99*, 1665−1688
(4) Grayson, S M ; Fréchet, J M J *Chem. Rev.* **2001**, *101*, 3819−3867
(5) Cölfen, H *Macromol. Rapid Commun.* **2001**, *22*, 219−252
(6) Allen, T M ; Cullis, P R *Science* **2004**, *303*, 1818−1822
(7) Broz, P ; Driamov, S ; Ziegler, J ; Ben-Haim, N ; Marsch, S ; Meier, W ; Hunziker, P *Nano Lett.* **2006**, *6*, 2349−2353
(8) Kunna, K ; Müller, C ; Loos, J ; Vogt, D *Angew. Chem.* **2006**, *118*, 7447−7450 Kunna, K ; Müller, C ; Loos, J ; Vogt, D *Angew. Chem., Int. Ed* **2006**, *45*, 7289−7292
(9) Fréchet, J M J *Proc. Natl. Acad. Sci. U.S.A.* **2002**, *99*, 4782−4787
(10) Chen, G -H ; Guan, Z -B *J. Am. Chem. Soc.* **2004**, *126*, 2662−2663
(11) Zheng, P -W ; Jiang, X -W ; Zhang, X ; Zhang, W -Q ; Shi, L -Q *Langmuir* **2006**, *22*, 9393−9396
(12) Lee, M ; Lee, S -J ; Jiang, L -H *J. Am. Chem. Soc.* **2004**, *126*, 12724−12725
(13) Gillies, E R ; Jonsson, T B ; Fréchet, J M J *J. Am. Chem. Soc.* **2004**, *126*, 11936−11943
(14) Sideratou, Z ; Tsiourvas, D ; Paleos, C M *Langmuir* **2000**, *16*, 1766−1769
(15) Barker, I C ; Cowie, J M G ; Huckerby, T N ; Shaw, D A ; Soutar, I ; Swanson L *Macromolecules* **2003**, *36*, 7765−7770
(16) Xu, J ; Luo, S -Z ; Shi, W -F ; Liu, S -Y *Langmuir* **2006**, *22*, 989−997
(17) Jia, Z -F ; Chen, H ; Zhu, X -Y ; Yan, D -Y *J. Am. Chem. Soc.* **2006**, *128*, 8144−8145
(18) Ma, Y -H ; Tang, Y -Q ; Billingham, N C ; Armes, S P ; Lewis, A L ; Lloyd, A W ; Salvage, J P *Macromolecules* **2003**, *36*, 3475−3484
(19) Berndt, I ; Popescu, C ; Wortmann, F -J ; Richtering, W *Angew. Chem.* **2006**, *118*, 1099−1102 Berndt, I ; Popescu, C ; Wortmann, F -J ; Richtering, W *Angew. Chem., Int. Ed.* **2006**, *45*, 1081−1085
(20) Cormia, R L ; Price, F P ; Turnbull, D *J. Chem. Phys.* **1962**, *37*, 1333−1340
(21) Ross, G S ; Frolen, L J *J. Res. Natl. Bur. Stand.* **1975**, *79A*, 701−711
(22) Hoffman, J D *Polymer* **1983**, *24*, 3−26
(23) Clausse, D *J. Therm. Anal.* **1998**, *51*, 191−201
(24) Montenegro, R ; Antonietti, M ; Mastai, Y ; Landfester, K *J. Phys. Chem. B* **2003**, *107*, 5088−5094
(25) Alakoskela, J -M I ; Kinnunen, P K J *J. Phys. Chem. B* **2001**, *105*, 11294−11301
(26) Reiter, G ; Castelein, G ; Sommer, J -U ; Röttele, A ; Thurn-Albrecht, T *Phys. Rev. Lett.* **2001**, *87*, 226101-1−226101-4

Scheme 1. Catalyst Precursors

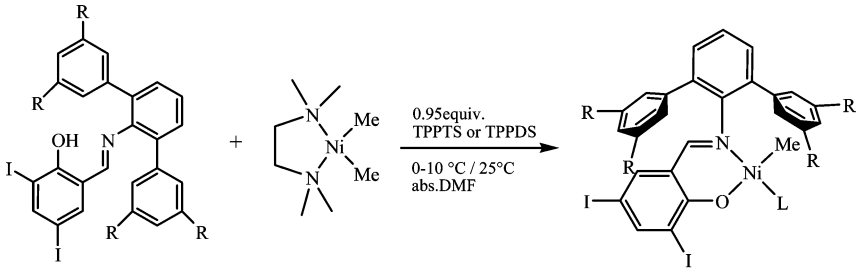

1: R = CF_3 , L =TPPTS
2: R = CH_3, L = TPPDS

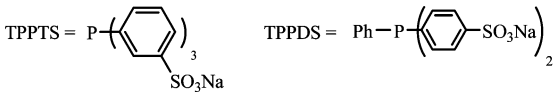

Table 1. Characterization Data of Dispersions I and II

dispersion	T_m/T_c in dispersion (°C)	T_m/T_c of bulk (°C)	crystallinity of bulk (%)[a]	methyl branching/ 1000 carbon atoms[b]	polymer solids content (wt %)[c]	M_n (M_w/M_n) (g/mol)[d]	size (nm)[e]	surface tension (mN/m)[f]
I	127/75	132/106	60	6	1.9	2×10^5 (2.4)	12	59
II	65/38	67/61	<20	50	2.2	1×10^4 (2.3)	9	62

[a] Determined by DSC. [b] Determined by ^{13}C NMR on the isolated bulk polymer. [c] Determined by precipitating the dispersions in methanol. [d] From GPC vs linear polyethylene. [e] Volume average size determined by DLS (173° single angle back scattering). [f] Of the as-prepared dispersions.

Table 2. Fluorescence Studies with Pyrene in Dispersions I and II[a]

sample	**I** − 1	**I** − 2	**I** − 3	**I** − 4	**I** − 5	**II** − 1	**II** − 2	**II** − 3	**II** − 4	**II** − 5
polyethylene conc (g/L)	0.017	0.119	0.924	2.86	10.98	0.014	0.094	0.703	2.09	8.61
mass ratio pyrene/polymer ($\times 10^{-3}$)	58	8	1	0.3	0.09	68	10	1	0.5	0.1
ratio pyrene molecules/polymer particles	150	21	2.7	0.87	0.23	71	11	1.4	0.48	0.12
I_3/I_1	0.62	0.76	0.79	0.83	0.94	0.68	0.89	0.93	0.98	1.08
I_3/I_1 (with added quencher DAE)		0.90	0.92	0.96			1.01	1.09	1.14	

[a] $C_{pyrene} = 4.7\ \mu mol\ L^{-1}$.

crystallization and melting in 10 nm polymer particles on the properties of guest probe molecules. The polymer polyethylene was employed. In terms of molecular structure, it is the simplest organic polymer, and its crystallization and structure in the bulk have been investigated more intensely than for any other polymer.[27] Also, as a hydrocarbon, polyethylene represents a highly lipophilic, apolar environment.

Results and Discussion

Aqueous solutions of nickel complex **1** polymerize ethylene to colloidally stable dispersions of particles of ∼10 nm size composed of linear semicrystalline polyethylene.[28] Branched ethylene homopolymers can also be obtained with late transition metal catalysts due to their chain running capability.[29,30] With water-insoluble catalysts related to **1**, the branching (and molecular weight) of the polymer could be varied over a wide range via the remote substituents R (Scheme 1).[31,32] For the present study, water-soluble **2** with remote substituents R = Me was prepared (Scheme 1).

Exposure of aqueous solutions of **2**, which also contained the surfactant sodium dodecyl sulfate (SDS) to stabilize polymer particles formed, to ethylene pressure at 15 °C afforded transparent colloidally stable dispersions of polyethylene particles of 10 nm volume average particle size as determined by dynamic light scattering (DLS; 173° backscattering), with a polymer solids content of 2.2 wt %. As anticipated, the dispersions formed with **2** (designated as dispersions **II**) are composed of highly branched polyethylene with 50 branches/1000 carbon atoms. Branch formation occurs via β-hydride elimination as a key step, which is also the key step for chain transfer.[31,33] Nonetheless, the polymers have a molecular weight of $M_n = 10^4$ g mol^{-1} (M_w/M_n = 2.3). This is sufficiently high to be in the regime where molecular weight has little influence on crystallization and crystallinity.[27] The bulk polymer melts at T_m = 67 °C (T_c = ∼60 °C) and possesses a crystallinity of ≤20% as determined by differential scanning calorimetry (DSC). By comparison, polymer dispersions obtained with **1** (dispersions **I**) employed for this study contained polyethylene with only 6 branches/1000 carbon atoms, $M_n = 2 \times 10^5$ g mol^{-1} (M_w/M_n = 2.4), bulk crystallinity = 60%, and T_m = 132 °C (T_c = 106 °C). Characterization data of dispersions **I** and **II** are summarized in Table 1.

A unique feature of the particles studied here is their small sizes, which are on the order of the smallest sizes observed for a polyethylene lamella to date.[34−37] The small sizes observed by

(27) Strobl, G R *The Physics of Polymers*, 2nd ed ; Springer: Berlin, 1997
(28) Göttker-Schnetmann, I ; Korthals, B ; Mecking, S *J. Am. Chem. Soc.* **2006**, *128*, 7708−7709
(29) Johnson, L K ; Killian, C M ; Brookhart, M *J. Am. Chem. Soc.* **1995**, *117*, 6414−6415
(30) Moehring, V M ; Fink, G *Angew. Chem.* **1985**, *97*, 982−984 Moehring, V M ; Fink, G *Angew. Chem., Int. Ed. Engl.* **1985**, *24*, 1001−1003
(31) Zuideveld, M A ; Wehrmann, P ; Röhr, C ; Mecking, S *Angew. Chem.* **2004**, *116*, 887−891 Zuideveld, M A ; Wehrmann, P ; Röhr, C ; Mecking, S *Angew. Chem., Int. Ed.* **2004**, *43*, 869−873
(32) Göttker-Schnetmann, I ; Wehrmann, P ; Röhr, C ; Mecking, S *Organometallics* **2007**, *26*, 2348−2362
(33) Jenkins, J C ; Brookhart, M *J. Am. Chem. Soc.* **2004**, *126*, 5827−5842
(34) Barham, P J ; Chivers, R A ; Keller, A ; Martinez-Salazar, J ; Organ, S J *J. Mater. Sci.* **1985**, *20*, 1625−1630

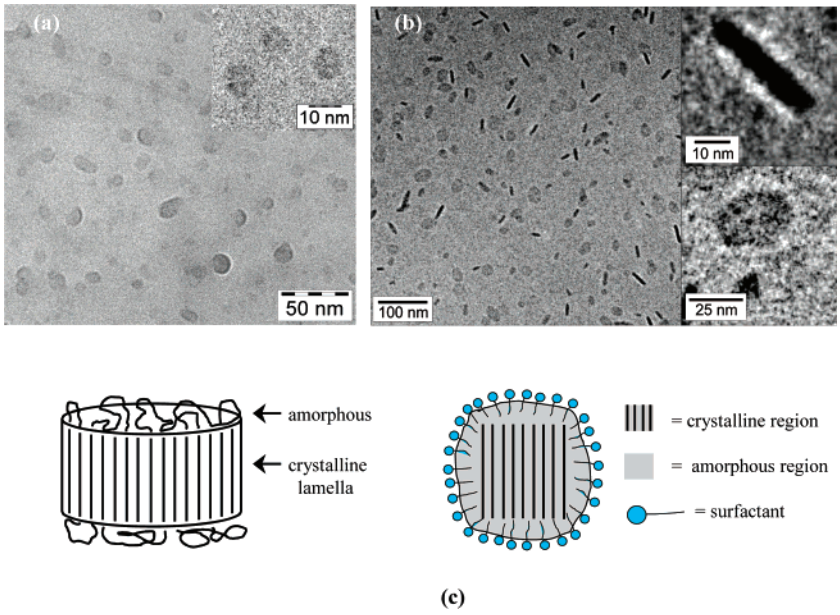

Figure 1. Cryo-TEM micrograph of polyethylene nanoparticles of (a) dispersion **II** and (b) dispersion **I** (from ref 38) for comparison. (c) Schematic structure of semicrystalline dispersed particles (**I**) of linear polyethylene.

DLS were confirmed by cryo-transmission electron microscopy (TEM). Small-angle X-ray scattering (SAXS) and cryo-TEM demonstrated the polyethylene particles in dispersion **I** to be single crystals, consisting of a lamella with a thickness of 6.3 nm sandwiched between two ~1 nm amorphous layers.[38,39] By comparison, cryo-TEM micrographs (Figure 1) show the particles of dispersion **II** to have a more spherical structure, as expected for less crystalline particles.

The dispersions can be heated to 140 °C without coagulation. Melt and crystallization transitions in the dispersed surfactant-stabilized particles were studied by differential scanning calorimetry (DSC) (Figure 2). In cooling traces, a high supercooling of crystallization is observed. Crystallization occurs at T_c = 75 °C and T_c = 38 °C for polymer dispersions **I** and **II**, respectively. This is due to crystallization of individual droplets versus heterogeneous nucleation in the bulk.[20−24]

The interaction of particles of variable crystallinity with probe molecules was studied by fluorescence spectroscopy over a range of particle number densities and ratios of probe to particle masses (Table 2 and Table S1 in the Supporting Information). Nile red (9-diethylamino-5*H*-benzo[alpha]phenoxazine-5-one) is a common lipophilic fluorescence probe.[40,41] In water, it is insoluble and does not fluoresce. In the presence of dispersed polyethylene nanoparticles, fluorescence was observed with the emission peak maximum located at around 646 nm (excitation with λ = 570 nm). The fluorescence intensity increases gradually with the concentration of polyethylene particles (Figure 3). By comparison, in SDS solutions of variable surfactant concentration, fluorescence was only observed above the critical micelle concentration (cmc) (Figure 3), as expected.[10] The dye can only be solubilized by SDS when free micelles are present. At the same mass concentrations, the absorbance in polyethylene dispersions is much

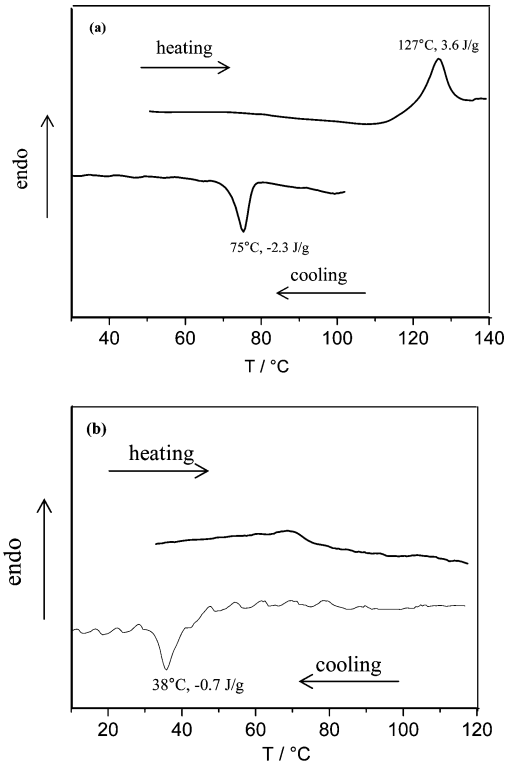

Figure 2. DSC traces of (a) dispersion **I** (2.3 wt % polymer solids content) and (b) dispersion **II** (4.0 wt %). Heating/cooling rate: 10 K min^{-1}.

higher than in SDS micelles (Figure S1 in the Supporting Information); that is, the polyethylene nanoparticles have a higher uptake capacity. Note that the dispersions as prepared have surface tensions of 60 mN m^{-1} and higher. This excludes any presence of free surfactant.

Pyrene has been used widely as a probe molecule which senses the polarity of its local environment.[42] The relative intensity of bands I_3/I_1 in fluorescence spectra is indicative of solvent polarity. We determined I_3/I_1 = 0.61 for water, 0.84 for methanol, 0.98

(35) Barham, P J ; Jarvis, D A ; Keller, A *J. Polym. Sci., Polym. Phys.* **1982**, *20*, 1733−1748
(36) Strobl, G *Eur. Phys. J. E* **2000**, *3*, 165−183
(37) Bauers, F M ; Thomann, R ; Mecking, S *J. Am. Chem. Soc.* **2003**, *125*, 8838−8840
(38) Weber, C H M ; Chiche, A ; Krausch, G ; Rosenfeldt, S ; Ballauff, M ; Göttker-Schnetmann, I ; Tong, Q ; Mecking, S *Nano Lett.* **2007**, *7*, 2024−2029
(39) Cheng, S Z D *Nature* **2007**, *448*, 1006−1007
(40) Greenspan, P ; Mayer, E P ; Fowler, S D *J. Cell Biol.* **1985**, *100*, 965−973
(41) Sackett, D L ; Wolff, J *Anal. Biochem.* **1987**, *167*, 228−234
(42) Kalyanasundaram, K ; Thomas, J K *J. Am. Chem. Soc* **1977**, *99*, 2039−2044

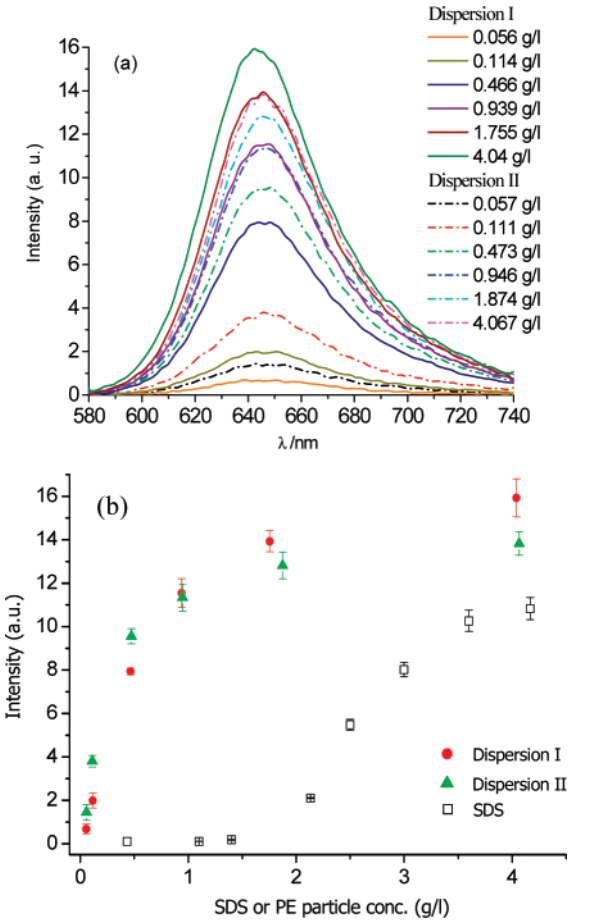

Figure 3. (a) Emission spectra of nile red in aqueous dispersions of polyethylene particles at variable particle concentrations (solid lines: dispersion **I**; dashed lines: dispersion **II**). (b) Fluorescence intensity at λ_{max} vs particle concentration, and vs SDS concentration for comparison.

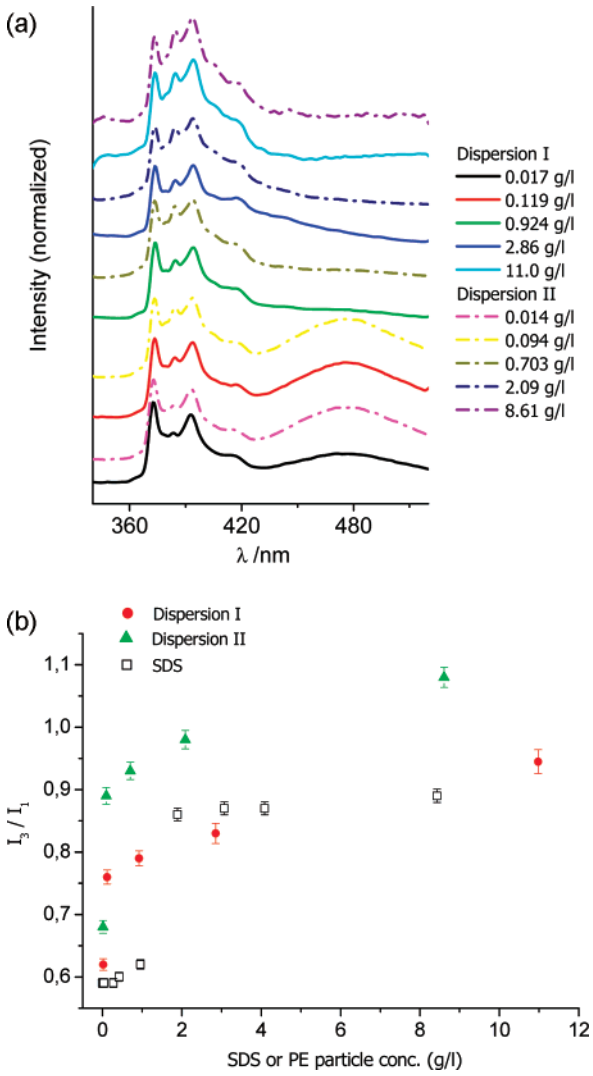

Figure 4. (a) Stacked plots of pyrene fluorescence intensities at different nanoparticle concentrations. Total amount of pyrene: 4.7 μmol L^{-1} = 0.95 mg L^{-1}. All spectra are normalized to the (0,0) peak at 374 nm. (b) I_3/I_1 ratios observed vs concentration of polyethylene dispersions, and vs SDS concentration for comparison. Total amount of pyrene: 4.7 μmol L^{-1} = 0.95 mg L^{-1}.

for *n*-butanol, and 1.60 for hexane and dodecane at 20 °C ([pyrene] = 4.7 μmol L^{-1}), which agrees with literature values.[42] In contrast to nile red, for pyrene, fluorescence is also observed for neat aqueous solutions. In the following fluorescence studies, potential contributions by pyrene dissolved in the aqueous phase must be considered.

The I_3/I_1 ratios increase gradually with polyethylene particle concentration at a given amount of pyrene present (Figure 4 and Table 2). At low particle concentrations, that is, at a high pyrene to particle ratio, excimer formation is observed. This confirms that more than one pyrene molecule can be present in a given particle. The presence or absence of excimer emission corresponds surprisingly well with the calculated ratio of the number of pyrene molecules present in the sample versus the number of polymer particles. Significant excimer formation is observed only at $N_{\text{pyrene molecules}}/N_{\text{particles}} > 1$. In contrast to the gradual increase of I_3/I_1 with increasing concentration of polyethylene particles, upon addition of SDS to a neat aqueous solution of pyrene, a significant change of I_3/I_1 is only observed at the cmc, as expected. Above the cmc, a threshold value of 0.9 is observed (Figure 4), in agreement with literature reports[42] (comparing this value with I_3/I_1 = 0.6 for aqueous solutions and I_3/I_1 = 1.6 for aliphatic hydrocarbon solvents indicates that in an SDS micelle (size = ~2−3 nm) pyrene (size = 0.8 nm) experiences an environment intermediate to water and hydrocarbons in polarity, corresponding rather to an interface than a hydrophobic "micelle core"). For the dispersions, I_3/I_1 ratios approach 0.95 and 1.1 for dispersions **I** and **II**, respectively. In the low crystalline particles, a less polar environment is experienced on average than in the crystalline particles. This is indeed due to the polarity experienced in the particles and not to a different partition ratio of pyrene between the particles and the aqueous phase, as evidenced by fluorescence studies in the presence of 0.15 mol L^{-1} 2-dimethylaminoethanol (DAE) as a water-soluble quencher (Table 2, entries **I**-2 to **I**-4 and **II**-2 to **II**-4). In aqueous solutions of pyrene in the absence of particles, at this quencher concentration, no significant fluorescence signals were observed. In the range of particle concentrations studied, the I_3/I_1 ratios observed are higher in the presence of quencher under otherwise identical conditions (Table 2). This shows that pyrene accessible to the quencher, that is, pyrene dissolved in the aqueous phase (or possibly also pyrene at the particle interface), contributes to the overall fluorescence signal detected in the absence of quencher.[43]

The temperature dependence of I_3/I_1 was studied. Samples were heated in closed cuvettes above the melting point of polyethylene. Fluorescence spectra were taken at different temperatures as the sample was gradually cooled to 25 °C (Figure 5). At high temperatures of 90−130 °C, for a given set of

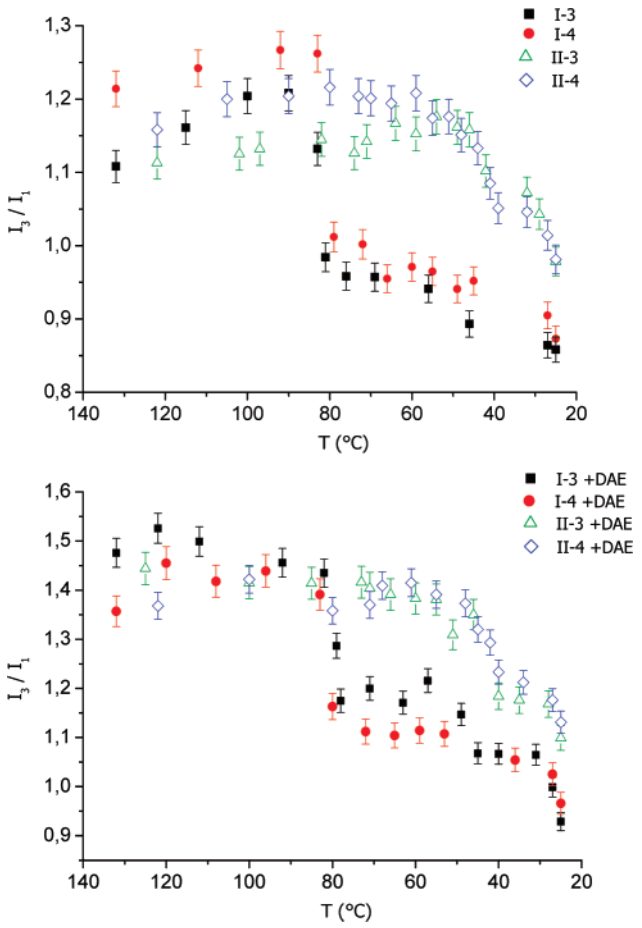

Figure 5. Temperature-dependent ratio of the intensity of fluorescence bands I_1 and I_3 (squares and circles: dispersions **I**, particle concentrations 0.924 and 2.86 g L^{-1}, respectively. Open triangles and diamonds: dispersions **II**, particle concentrations 0.703 and 2.09 g L^{-1}, respectively. Total amount of pyrene: 4.7 μmol L^{-1} in all cases). Bottom graph: Same as above but in the presence of 0.15 mol L^{-1} DAE quencher.

conditions, the I_3/I_1 ratio is similar for dispersions **I** (of linear polymer) and **II** (of branched polymer), as should be expected when the polymers are in the molten noncrystalline state. Particularly, in the presence of DAE quencher, in which case a contribution from the aqueous phase is suppressed, I_3/I_1 ratios around 1.5 were observed at $T > 90$ °C, which are close to the value of the low molecular weight aliphatic hydrocarbon solvents of 1.6.

Upon cooling of the dispersions, a pronounced jump of I_3/I_1 occurs. The temperature at which the jump occurs coincides within experimental error with the crystallization temperatures ($T_c = 75$ and 38 °C for dispersions **I** and **II**, respectively) observed by DSC on the different dispersions. Note that DSC studies on dispersion **I** revealed no strong effect of the presence or absence of pyrene on the crystallization temperature (cf. Figure S2 in the Supporting Information). The jump in I_3/I_1 at the crystallization temperature also occurs in the presence of quencher. The observed jump therefore cannot be related solely to a conceivable change in partioning of the dye between the particles and the aqueous phase upon crystallization, that is, an expulsion of the dye from the particles by crystallization. Rather, the dye in the particles experiences a change in the average environment encountered. In a crystallized particle of the very small size studied here, the amorphous phase in which the dye can be solubilized is located entirely at the periphery of the particle (Figure 1) such that it will experience the particle−water interface to a certain extent as outlined above.

Studies of the dispersions by DLS after cooling to room temperature showed that no coagulation has occurred during the melting/recrystallization cycle. At room temperature, the original fluorescence spectrum observed prior to the melting/crystallization cycle is resumed.

Summary and Conclusions

Aqueous dispersions of very small particles of ~10 nm size composed of polyethylene with a highly variable degree of branching and crystallinity are accessible by catalytic polymerization of ethylene with appropriate water-soluble Ni(II) complexes. Fluorescence studies show that the particles take up lipophilic molecules such as nile red or pyrene. Studies of pyrene fluorescence reveal that in the particles pyrene experiences a rather apolar environment. However, the polarity experienced does not quite reach that of aliphatic hydrocarbon solvents or of polymer melts (the latter dispersed as 10 nm droplets). This shows that pyrene molecules in the particles sense the surfactant-covered water−particle interface to some extent (possibly via short-range penetration of water or the surface charge[42]). This effect is significantly more pronounced for crystalline particles, in which amorphous polymer portions which accommodate the probe molecules can only be located at the periphery. In the low crystalline particles, the pyrene molecules experience a less polar environment on average. The polarity experienced by the probe molecules in these nanoscale compartments can be switched reversibly by crystallization in the particles, which is induced by a temperature change. The crystallization temperature at which this occurs depends on the degree of branching of the polymer and can thus be controlled via the latter. Such nanocontainers with uptake properties tunable by crystallinity, and which can be switched via crystallization are unprecedented. At the same time, the system studied is conveniently accessible from ethylene as a readily available building block.

Experimental Section

Materials and General Considerations. Unless noted otherwise, all manipulations of nickel complexes were carried out under an inert atmosphere using a glovebox or standard Schlenk techniques. All glassware was flame-dried under vaccum before use. Toluene and pentane were distilled from sodium, and diethylether was distilled from sodium/benzophenone under argon. Demineralized water was distilled under nitrogen and degassed three times after distillation. Dimethylformamide (DMF) was thoroughly degassed by several freeze−pump−thaw cycles and stored in a glovebox. [(tmeda)$NiMe_2$] was supplied by MCAT (Konstanz, Germany). TPPTS (Aldrich, 96%), SDS (Fluka, 98%), nile red (Fluka, 99%), and pyrene (Aldrich, 99%) were used as received. TPPDS was prepared according to ref 44. Ni(II) complex **1** was prepared as reported previously.[28]

NMR spectra were recorded on a Varian Unity INOVA 400 spectrometer or on a Bruker AC 250 spectrometer. ^{1}H NMR and ^{13}C NMR chemical shifts were referred to the solvent signal. High-temperature NMR measurements of polyethylenes were performed in 1,1,2,2-tetrachloroethane-d_2 at 120 °C. The branching structure was assigned according to refs 45 and 46. Elemental analyses were

(43) In detail, the I_3 / I_1 ratio observed in the presence of quencher is not constant but also increases somewhat with particle concentration (at a fixed amount of pyrene present in the sample; cf Table 1) This implies that the average environment experienced by the pyrene probe located in the particles changes with particle concentration; that is, at higher polymer particle/ pyrene ratios, the portion of pyrene located at the interface versus the interior of the particles decreases

(44) Herd, O ; Heβler, A ; Langhans, K P ; Stelzer, O ; Sheldrick, W S ; Weferling, N *J. Organomet. Chem.* **1994**, *475*, 99−111
(45) Randall, J C *J. Macromol. Sci., Rev. Macromol. Chem. Phys.* **1989**, *C29*, 201−317

performed up to 950 °C on an Elementar Vario EL instrument. Differential scanning calorimetry was performed on a Netzsch Phoenix 204 F1 at a heating and cooling rate of 10 K min^{-1}. DSC data reported for bulk polymers are from the second heating cycles. Polymer crystallinities were calculated based on a melt enthalpy of 293 J g^{-1} for 100% crystalline polyethylene. DSC traces of dispersions were obtained on ∼15 mg of dispersion with approximately 2 and 4 wt % polymer solids content for dispersions **I** and **II**, respectively. Gel permeation chromatography (GPC) was carried out in 1,2,4-trichlorobenzene at 160 °C on a Polymer Laboratories 220 instrument equipped with Mixed Bed PL-columns. Data reported were referenced to linear polyethylene standards. Dynamic light scattering was performed on a Malvern NanoZS ZEN 3600 particle sizer (173° backscattering) on diluted dispersions. The autocorrelation function was analyzed using the Malvern dispersion technology software 3.30 algorithm to obtain volume and number weighted particle size distributions.

Synthesis and Characterization of Catalyst Precursor 2. To a mixture of [(tmeda)$NiMe_2$] (22.4 mg, 110 μmol) and 100 μmol salicylaldimine 6-[C(H)═N{2,6-(3,5-$Me_2C_6H_3)_2C_6H_3$}]-2,4-$I_2C_6H_2$-OH[31] in a septum capped Schlenk tube was added DMF (2.0 mL) via syringe at 20 °C with stirring under nitrogen. Rapid reaction was evident by the fast evolution of methane which ceased within 5 min. The resulting orange to red solution was stirred for 10 min at 20 °C, TPPTS or TPPDS (90 μmol) and DMF (1 mL) were added, and the mixture was stirred for an additional 30 min. The solvent was carefully removed under high vacuum (10^{-3} mbar), and the residue was suspended in diethyl ether (5 mL) and then transferred to a gastight centrifugation vial. The suspension was repeatedly centrifuged, the supernatant was removed, and the orange solid was redispersed with 5 mL portions of diethyl ether until the supernatant remained nearly colorless. Complex **2** was obtained as the DMF adduct after removal of the residual solvent under high vacuum (10^{-3} mbar) in 90% yield. ^{1}H NMR (399.8 MHz, CD_3OD, 298 K): δ 8.04 (s, 1H, DMF), 7.85 (d, $^4J_{PH}$ = 8.0 Hz, 1H, 7-H), 7.75 (m, 4H, TPPDS), 7.63 (d, $^4J_{HH}$ = 2.0 Hz, 1H, 4-H), 7.56 (m, 6H, TPPDS), 7.31 (m, 6H, 10−12-H and TPPDS), 7.12 (s, 4H, 15-, 19-, 21-, 25-H), 7.06 (d, $^4J_{HH}$ = 2.0 Hz, 1H, 6-H), 7.02 (s, 2H, 17-, 23-H), 2.95 (s, 3H, DMF), 2.82 (s, 3H, DMF), 2.30 (s, 12H, 26−29-H), −1.46 (d, $^3J_{PH}$ = 7.2 Hz, 3H, Ni−CH_3). ^{31}P{^{1}H} NMR (161.8 MHz, CD_3OD, 298 K): δ 30.7. Elemental analysis calculated for **2**·DMF $C_{51}H_{47}N_2O_8S_2I_2Na_2PNi$ (molecular weight = 1269.5 g mol^{-1}): C, 48.25; H, 3.73; N, 2.21. Found: C, 46.92; H, 3.40; N, 1.93.

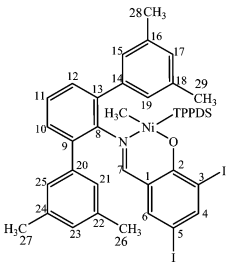

Dispersion Synthesis.[28] Dispersion synthesis was carried out in a 300 mL stainless steel mechanically stirred (1000 rpm) pressure reactor equipped with a heating/cooling jacket supplied by a thermostat controlled by a thermocouple dipping into the polymerization mixture. To a mixture of 750 mg of SDS and 10 μmol of the respective complex in a 250 mL Schlenk flask was added 100 mL of distilled and degassed water at room temperature. The resulting homogeneous solution was then cannula-transferred to the argon flushed reactor cooled to 12 °C. The reactor was pressurized to a constant pressure of 40 bar ethylene while the temperature was adjusted to 15 °C. After 30 min reaction time, ethylene feeding was interrupted, the reactor was carefully depressurized, and the obtained dispersion was filtrated through a plug of glass wool. To determine the solids content, an aliquot of 20 g of dispersion was precipitated with 150 mL of MeOH. The obtained bulk polymer was filtrated and thoroughly washed with MeOH and H_2O and then dried under vaccum at 50 °C overnight.

Cryo-TEM. The electron microscopic investigations were performed on a Zeiss Libra 120 transmission electron microscope operated at 120 kV acceleration voltage. For cryo-TEM, a Gatan CT3500 cryo-transfer system was used. Specimens for the cryo-TEM investigations were prepared by freezing a thin film of the suspension in liquid ethane. The thin film was created by dripping a small amount of the suspension on a 700 mesh grid. A meniscus, thin enough for use in TEM, forms over the holes in the grid and is rapidly frozen to give a vitrified sample. The sample was then cryo-transferred into the TEM and examined at a temperature around 90 K with minimal electron dose.

Fluorescence Studies. All fluorescence and absorption studies are based on at least two independent experiments. Steady-state fluorescence measurements were carried out on a Perkin-Elmer LS 50 luminescence spectrometer. The samples were excited at 333 and 570 nm for the cases of pyrene and nile red, respectively. The spectra were recorded with a slit width of 2.5 nm and scanning speed of 100 nm min^{-1}. All UV/vis absorption spectra were recorded on a Perkin-Elmer Lambda 18 UV/vis dual-beam spectrometer with distilled water as a reference.

A general prerequisite for these studies is that with increasing particle number density multiple scattering in the sample does not deteriorate detection of the fluorescence signal. This was fulfilled under all conditions studied. Spot tests in which fluorescence spectra were taken repeatedly on a given sample showed the results to be time-independent; that is, it can be safely assumed that the systems reach a constant state rapidly.

Reported values for the solubility of pyrene in water vary.[42,47] We determined a saturation concentration of ∼4 μmol L^{-1} at 20 °C.

A stock solution of pyrene (0.096 g L^{-1}, 0.47 mM) in MeOH was prepared via sonication. Different amounts of polyethylene dispersions were diluted with water to desired concentrations. The resulting samples were added to the same amount of pyrene stock solution and kept at room temperature overnight to reach equilibrium. The final samples contain 4.7 μM pyrene and 1 vol % MeOH. This amount of MeOH has no influence on the fluorescence of pyrene, as confirmed by measuring the fluorescence of pyrene in different solvent mixtures of MeOH and H_2O. The pyrene-to-polyethylene particle ratio was varied from approximately 100−0.1 (Table 1).

Similar results as with 2-dimethylaminoethanol (DAE) as a quencher were obtained with 0.05 mol L^{-1} solutions of KI as a quencher. DAE was preferred, however, as the addition of KI and resulting increased ionic strength of the solution which decreases electrostatic stabilization sometimes resulted in partial coagulation of the particles, as observed by DLS.

For temperature-varied fluorescence measurements, the samples were heated externally in a closed fluorescence cell up to 133 and 120 °C for dispersions **I** and **II**, respectively. After equilibration at this temperature for ∼2 min, the samples were transferred to a thermostated cell holder in the UV/vis spectrometer which was preheated to 95 °C. The emission spectra were recorded successively until reaching a stable state within ∼6 min. The samples were then allowed to cool down to room temperature within ∼30 min, and the emission spectra were recorded while cooling. The sample temperature was measured with a thermocouple dipping into the sample directly before each recording of the emission spectra.

As for the temperature dependence of the I_3/I_1 ratios, for the pyrene solution in dodecane ([pyrene] = 4 μmol L^{-1}), the I_3/I_1 ratio did not vary significantly with temperature in the range studied, and also for the aqueous pyrene solution temperature only had a slight effect, I_3/I_1 = 0.6−0.7.

An aqueous dispersion of nile red (0.016 g L^{-1}) was prepared via sonication. Different amounts of polyethylene dispersions were then added to 3 mL each of this nile red aqueous dispersion. The resulting samples were stored at room temperature, and the fluorescence and

(46) Axelson, D E ; Levy, G C ; Mandelkern, L *Macromolecules* **1979**, *12*, 41−52

(47) Cao, T ; Munk, P ; Ramireddy, C ; Tuzarlt, Z ; Webber, S E *Macromolecules* **1991**, *24*, 6300−6305

UV/vis absorption spectra were recorded until the dispersions were saturated with nile red, as indicated by no further change in absorbance occurring. The absorption peaks in the UV/vis spectra are located at 575 and 580 nm in the nanoparticle dispersions and SDS micelles, respectively.

Acknowledgment. Financial support by the DFG (international research training group "soft condensed matter") and by the BMBF (project 03X5505) is gratefully acknowledged. S.M. is indebted to the Fonds der Chemischen Industrie and to the Hermann−Schnell Foundation.

Supporting Information Available: DSC, DLS, GPC, and fluorescence data. This material is available free of charge via the Internet at http://pubs.acs.org

LA702500N